JACS
JOURNAL OF THE AMERICAN CHEMICAL SOCIETY
Article
pubs.acs.org/JACS

Ethylenediamine Promotes Cu Nanowire Growth by Inhibiting Oxidation of Cu(111)

Myung Jun Kim,[†] Patrick F. Flowers,[†] Ian E. Stewart,[†] Shengrong Ye,[†] Seungyeon Baek,[‡] Jae Jeong Kim,[‡] and Benjamin J. Wiley*[,†]

[†]Department of Chemistry, Duke University, 124 Science Drive, Box 90354, Durham, North Carolina 27708, United States
[‡]School of Chemical and Biological Engineering, Seoul National University, Seoul 151-742, Republic of Korea

Supporting Information

ABSTRACT: The synthesis of metal nanostructures usually requires a capping agent that is generally thought to cause anisotropic growth by blocking the addition of atoms to specific crystal facets. This work uses a series of electrochemical measurements with a quartz crystal microbalance and single-crystal electrodes to elucidate the facet-selective chemistry occurring in the synthesis of Cu nanowires. Contrary to prevailing hypotheses, ethylenediamine, a so-called capping agent in the synthesis of Cu nanowires, causes anisotropic growth by *increasing* the rate of atomic addition to (111) facets at the end of a growing nanowire relative to (100) facets on the sides of a nanowire. Ethylenediamine increases the reduction rate of $Cu(OH)_2^-$ on a Cu(111) surface relative to Cu(100) by selectively inhibiting the formation of Cu oxide on Cu(111). This work demonstrates how studying facet-selective electrochemistry can improve the understanding of the processes by which atoms assemble to form anisotropic metal nanostructures.

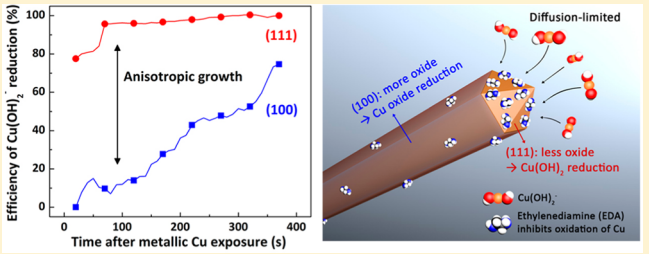

INTRODUCTION

One-dimensional nanowires of gold (Au), silver (Ag), and copper (Cu) have been extensively researched owing to their size-dependent electrical, catalytic, mechanical, and optical properties.[1−9] Cu nanowires are of particular interest due to the relatively large abundance of Cu, its low cost, and its high electrical and thermal conductivities.[10−12] For example, solution-deposited networks of Cu nanowires potentially offer a low-cost alternative to vapor-deposited indium tin oxide (ITO) as the transparent conductor[13−15] in solar cells,[16,17] organic light-emitting diodes (OLEDs),[18] touch screens,[19] and electrochromic windows.[20] Whereas ITO is brittle, composites of Cu nanowires in an elastomer exhibit little deterioration of their electrical conductivity after mechanical bending and stretching, demonstrating their potential for flexible and stretchable electronics.[18,21,22] The use of Cu nanowires has also been demonstrated in a variety of electrochemical applications, including batteries,[23−25] electrocatalysts,[26−28] and sensors.[29]

Cu nanowires have been synthesized by chemical vapor deposition,[30] a template-assisted method,[31] electrospinning,[32] and several solution-phase syntheses.[33−38] Among these methods, the low-temperature solution-phase synthesis is perhaps the simplest method and has been scaled up to produce grams of Cu nanowires.[35] The solution for the synthesis of Cu nanowires consists of a metal precursor, a reducing agent, and a so-called capping agent (i.e., a ligand that selectively blocks a particular facet or group of facets).[11,12,34−38] The oxidation of the reducing agent provides electrons for the reduction of the metal precursor, and the capping agent directs the growth of the metal nanostructure into nanowires instead of nanoparticles.

The formation of Cu nanowires is due to the difference in the growth rate of the Cu crystals along different crystallographic directions.[11,12] Cu nanowires grow to be tens of micrometers long via the selective reduction of ionic Cu species onto the end of the nanowires, which consists of a pentagonal pyramid with five (111) planes.[11,12,39] In comparison, the addition of Cu to the (100) planes on the sides of the nanowire is so minimal that the diameters of the nanowires are typically between 20 and 150 nm.[11,12,15,34] It has been hypothesized that the difference in the observed growth rate between the (100) and (111) planes may be due to the capping agent preferentially adsorbing on the (100) surface and physically blocking the addition of Cu to that surface.[11,12,37,40] Similar hypotheses have been suggested to account for the growth of Ag and Au nanowires in the presence of capping agents.[2,4−6] The capping agents for the syntheses of Cu nanowires usually have an amine functional group and include such chemicals as ethylenediamine (EDA),[19,34,37−40] hexadecylamine (HDA),[36,41,42] and octadecylamine (ODA).[43]

In principle, the difference in atomic addition to different facets due to the presence of a capping agent can be measured with appropriate electrochemical measurements on Cu(111) and Cu(100) single crystals in the reaction solution. This article

Received: October 11, 2016
Published: December 15, 2016

© 2016 American Chemical Society

DOI: 10.1021/jacs.6b10653
J. Am. Chem. Soc. 2017, 139, 277−284

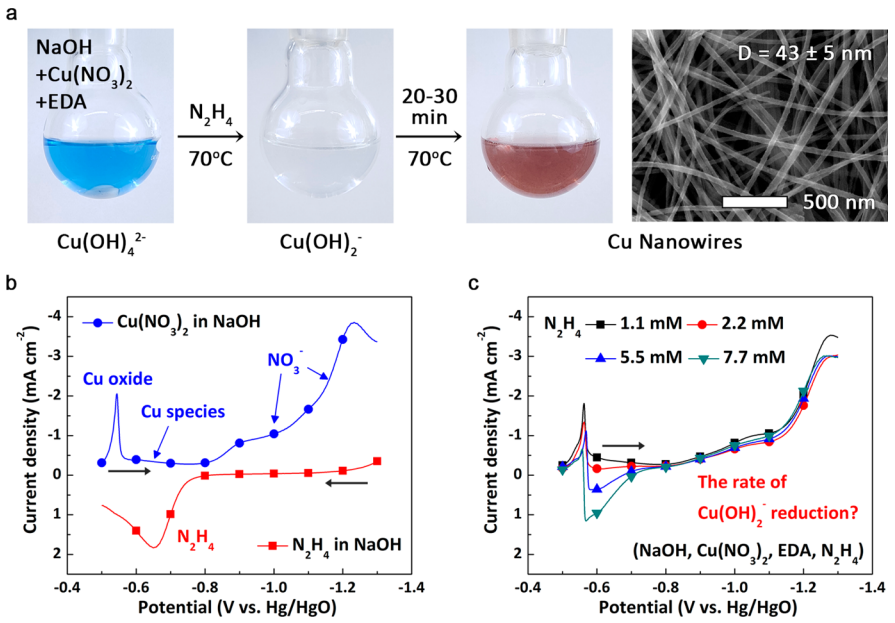

Figure 1. (a) Stages of the Cu nanowire synthesis. *I*–*V* curves for a polycrystalline Cu electrode in 15 M NaOH solutions (b) with either 4.74 mM $Cu(NO_3)_2$ (blue circles) or 5.5 mM N_2H_4 (red squares) and (c) with 70 mM EDA, 4.74 mM $Cu(NO_3)_2$, and various concentrations of N_2H_4. The direction of the linear potential sweeps is indicated with black arrows.

reports the first such experiments and demonstrates that although EDA does promote the growth of Cu nanowires, it does not do so in the way that has previously been hypothesized. Rather than blocking electrochemical reactions from happening on (100) facets, EDA preferentially promotes reduction of $Cu(OH)_2^-$ on (111) facets by keeping them relatively free of Cu oxide. It is the presence of Cu oxide on (100) facets that hinders atomic addition to the sides of the nanowire. Thus, we show that EDA is a facet-selective promoter of Cu nanowire growth rather than a true capping agent. A similar electrochemical approach can likely be applied to a variety of metal nanostructure syntheses to determine the precise role of so-called capping agents and thereby greatly improve the understanding of how such nanostructures form.

RESULTS AND DISCUSSION

Identification of Relevant Electrochemical Reactions. Prior to clarifying the role of EDA, it is important to establish the basic characteristics of the electrochemical reactions in the Cu nanowire synthesis. The synthesis of Cu nanowires is performed by a sequential addition of $Cu(NO_3)_2$, EDA, and N_2H_4 in concentrated NaOH solution (Figure 1a). When Cu ions were introduced to the NaOH solution, the solution color turned blue and remained this color after EDA was added. Previously, it was confirmed that this blue color is due to the formation of $Cu(OH)_4^{2-}$ instead of a Cu–EDA complex.[40] After heating the solution at 70 °C and adding N_2H_4 as the reducing agent, the solution became colorless and bubbles formed due to the reduction of divalent $Cu(OH)_4^{2-}$ to monovalent $Cu(OH)_2^-$ by N_2H_4. After 20–30 min at 70 °C, the color of the solution changed to a copper color due to the formation of Cu nanowires via the reduction of $Cu(OH)_2^-$ to metallic Cu.

The growth of Cu nanowires depends on two redox reactions: the oxidation of N_2H_4 and the reduction of ionic Cu species. In addition, a surface oxide can be continuously produced on the Cu nanowires due to a large amount of OH^- in the reaction solution;[44] this surface oxide is in turn reduced by N_2H_4. These reactions can be observed in Figure 1b, which shows *I*–*V* curves for a polycrystalline Cu electrode in NaOH solutions with either $Cu(NO_3)_2$ or N_2H_4. For oxidation, a single peak near −0.65 V vs Hg/HgO was assigned to N_2H_4 oxidation due to the linear relationship between the concentration of N_2H_4 and the peak current density (see Figure S1). For reduction, the polarization curve shows that four reactions could take place. The first sharp peak around −0.52 V is due to the reduction of surface oxide on the Cu electrode. Strong support for this assignment comes from the fact that such a peak was observed in the NaOH solution without any reagents (see Figure S2a). This peak nearly disappeared after the first voltage sweep because the majority of surface oxide was removed during the first sweep. The small current between −0.6 and −0.8 V is due to the reduction of ionic Cu species ($Cu(OH)_4^{2-}$, $Cu(OH)_2^-$), and the broad peaks over −0.8 V are due to the reduction of NO_3^-. Evidence for these assignments was obtained by comparing the polarization curves for NaOH solutions containing $Cu(NO_3)_2$, $CuSO_4$, and $NaNO_3$ (see Figure S2b).

The change in the solution color suggests that $Cu(OH)_2^- + e^- \rightarrow Cu + 2OH^-$ is the main reduction reaction for Cu nanowire growth[40] and that the oxidation of N_2H_4 ($N_2H_4 + 4OH^- \rightarrow N_2(g) + 4H_2O + 4e^-$)[45] provided electrons for this reduction reaction. Therefore, the most direct way to clarify the effect of EDA on Cu nanowire growth would be to measure the reduction rate of $Cu(OH)_2^-$ with different concentrations of EDA. However, in order to make $Cu(OH)_2^-$, it is necessary to add N_2H_4 because the reduction of $Cu(OH)_4^{2-}$ to $Cu(OH)_2^-$ requires one electron. Figure 1c shows that the current for N_2H_4 oxidation overlaps with the current associated with reduction of $Cu(OH)_2^-$, meaning that the usual linear sweep and cyclic voltammetry cannot distinguish between the currents that arise from the reduction of $Cu(OH)_2^-$ and the oxidation of N_2H_4.

DOI: 10.1021/jacs.6b10653
J. Am. Chem. Soc. 2017, 139, 277–284

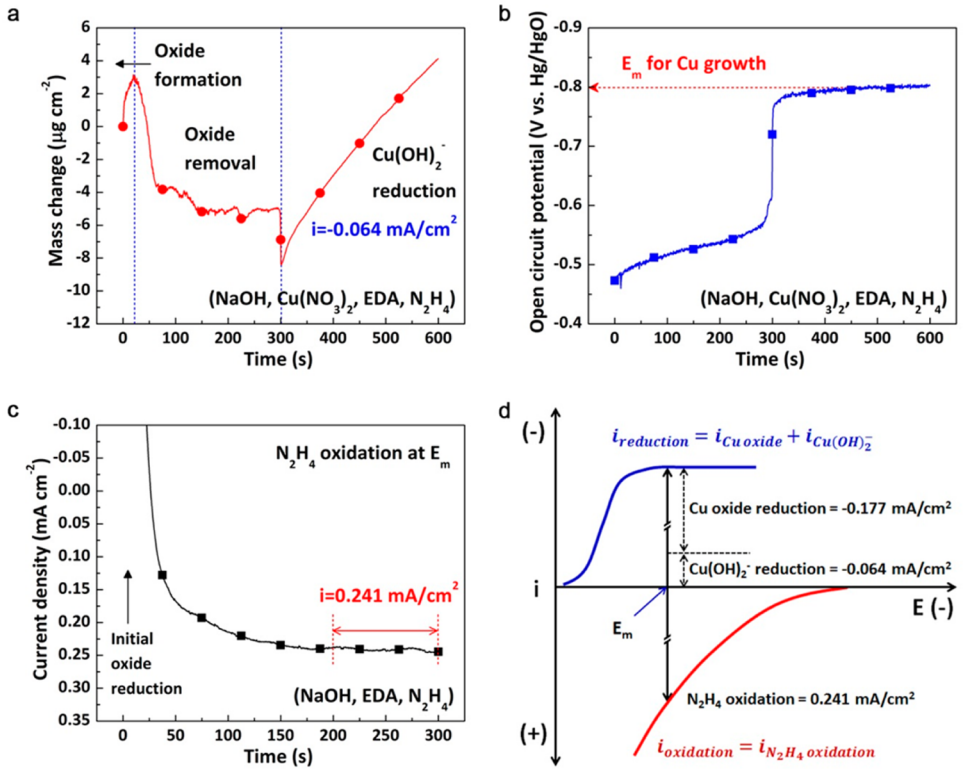

Figure 2. Changes in (a) mass and (b) open circuit potential at a polycrystalline Cu electrode in 15 M NaOH solution with 4.74 mM $Cu(NO_3)_2$, 70 mM EDA, and 5.5 mM N_2H_4. (c) Current−time behavior for N_2H_4 oxidation at E_m on polycrystalline Cu in a 15 M NaOH solution with 70 mM EDA and 5.5 mM N_2H_4. (d) Diagram of redox reactions in the Cu nanowire growth solution.

Determination of the Electrochemical Potential and Redox Currents for Nanowire Growth. To separately determine the currents from reduction of $Cu(OH)_2^-$ and oxidation of N_2H_4, we used an electrochemical quartz crystal microbalance (EQCM) to simultaneously measure the changes in mass and reaction potential at an electrode in the nanowire growth solution. According to mixed potential theory, spontaneous redox reactions occur at a mixed potential (E_m) where their rates are identical.[46,47] For Cu nanowire growth, the redox reactions take place at a potential where the cathodic current from the reduction of Cu species exactly matches the anodic current from the oxidation of N_2H_4. Thus, the current from oxidation of N_2H_4 at this potential can be used for estimating the reduction rate of Cu species. In addition, the change in the mass of the electrode can be used to calculate the current due to reduction of $Cu(OH)_2^-$. Comparing the reduction rate of $Cu(OH)_2^-$ calculated from the mass change and the oxidation rate of N_2H_4 at the reaction potential shows that most of the electrons from N_2H_4 oxidation go toward reduction of Cu oxide.

The mass and potential behaviors of a polycrystalline Cu electrode in the solution for nanowire synthesis are presented in Figure 2a,b. Initially, the electrode mass increased for 20 s due to the rapid formation of surface oxide in a high pH environment.[44] The mass then decreased for 280 s due to the reduction of the oxide by N_2H_4. These steps took place at a potential below −0.55 V (Figure 2b). At t = 300 s, a sharp decrease in the mass and a shift in the potential from −0.55 to −0.75 V were observed due to the exposure of metallic Cu. Finally, the mass of the electrode started to increase, implying Cu deposition on the electrode. The increase in the mass during this period gave an average reduction rate for $Cu(OH)_2^-$ of −0.064 mA/cm^2. At the same time, the potential stabilized to a value of −0.8 V, which was used as the E_m for the spontaneous redox reactions on a polycrystalline Cu electrode.

The oxidation rate of N_2H_4 at E_m was obtained from chronoamperometry in a NaOH solution containing EDA and N_2H_4 (Figure 2c), and the average current of N_2H_4 oxidation was found to be 0.241 mA/cm^2. This value is 3.77 times greater than the reduction current of $Cu(OH)_2^-$ calculated from the mass change, suggesting that a large amount of electrons from N_2H_4 were continuously consumed by the reduction of Cu oxide. Figure 2d summarizes the redox reactions on the Cu surface and illustrates how the combined current going to reduction of both Cu oxide and $Cu(OH)_2^-$ equals the current from oxidation of N_2H_4. The difference between the oxidation rate of N_2H_4 (Figure 2c) and the reduction rate of $Cu(OH)_2^-$ (Figure 2a) is equal to the reduction rate of Cu surface oxide, which was −0.177 mA/cm^2. This implies that reduction of Cu oxide and $Cu(OH)_2^-$ competitively occurs on the electrode and consumes 73.4 and 26.6% of the electrons provided by N_2H_4 oxidation, respectively. These results suggest that the formation of surface oxide by OH^- and its reduction by N_2H_4 are important to Cu nanowire growth.

Comparing the EDA-Dependent Electrochemistry of Cu(111) and Cu(100) Single-Crystal Electrodes. It has previously been shown that the structure of synthesized Cu nanowires is 5-fold twinned such that the sides of the nanowire consist of (100) planes and the end is capped with a pentagonal pyramid consisting primarily of (111) planes.[11,12,39,40] It has been hypothesized that the adsorption of EDA on (100) facets results in anisotropic growth by preferentially capping the side of the Cu nanowire. Therefore, the role of EDA was investigated with two Cu single crystals, oriented and polished

DOI: 10.1021/jacs.6b10653
J. Am. Chem. Soc. 2017, 139, 277−284

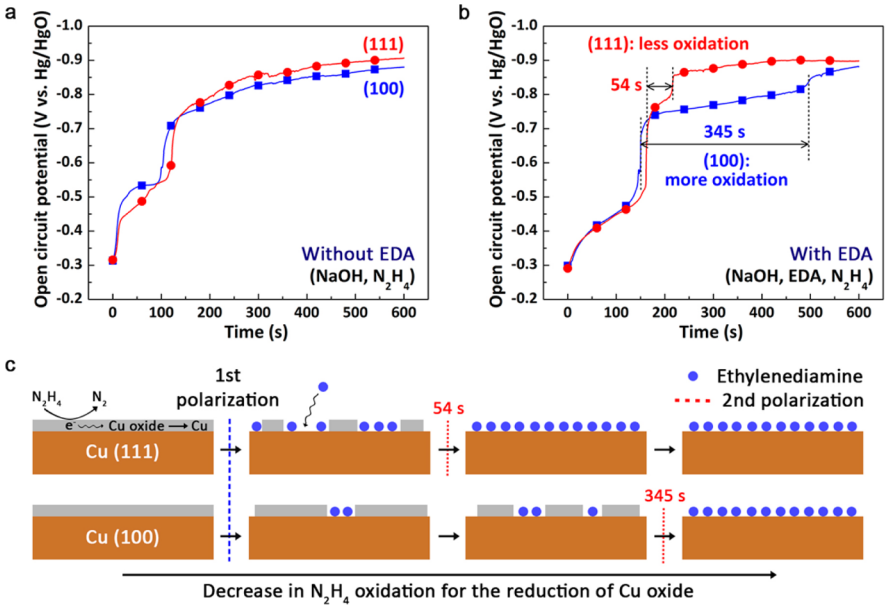

Figure 3. Potential behavior of Cu(100) and Cu(111) electrodes in 15 M NaOH solutions containing 5.5 mM N_2H_4 (a) without and (b) with 70 mM EDA. (c) Schematic diagram of Cu(111) and Cu(100) surfaces in a NaOH–EDA–N_2H_4 solution showing the removal of Cu oxide and the adsorption of EDA.

to show either the (100) or (111) surface. Since the reduction of surface oxide plays an important role in Cu nanowire growth, we first examined the open circuit potential of Cu(100) and Cu(111) crystals in NaOH–N_2H_4 solutions with and without EDA.

In the absence of EDA (Figure 3a), we observed a decrease in the potential over time that was roughly the same for both Cu(111) and Cu(100) electrodes. This decrease in potential corresponds to a decrease in the current from the oxidation of N_2H_4 and reduction of surface oxide. We believe that the rapid polarization occurring around 150 s, as with the similar potential change in Figure 2b, is associated with the partial exposure of the metallic Cu surface. In the presence of EDA, a second smaller polarization was observed, and this potential shift to −0.9 V occurred much more rapidly for Cu(111) than for Cu(100). It took only 54 s for the potential to drop to −0.9 V for Cu(111) after the first polarization, compared to 345 s for Cu(100). The oxidation rate of N_2H_4 is essentially zero at −0.9 V (see Figure 1b), meaning that the surface oxide is completely removed and no new oxide is being generated. Our interpretation of these results is shown in Figure 3c. After the first polarization, EDA started to adsorb on the surface of the metallic Cu and inhibit its further oxidation. Since EDA adsorbed more quickly on (111) than on (100), there was a period during which the surface oxide was completely removed on the (111) surface while the (100) surface was still oxidized.

The inhibition of surface oxidation by EDA suggests that EDA might also hinder electrochemical reactions from occurring on the electrode. To determine if this was the case, we measured the current from oxidation of N_2H_4 versus EDA concentration (Figure 4). Surprisingly, the peak current for N_2H_4 oxidation *increased* with an increase in EDA concentration. EDA promoted the oxidation of N_2H_4, likely by keeping the electrode surface metallic and free of oxide. This means that EDA does not behave like a traditional capping agent in that it does not physically block the approach of electrochemical reactants. In addition, the oxidation current of N_2H_4 was greater on Cu(111) than on Cu(100), indicating that EDA promotes the oxidation of N_2H_4 to a greater extent on (111) facets. These results suggest that EDA promotes anisotropic growth of Cu nanowires by keeping the (111) facets at the end

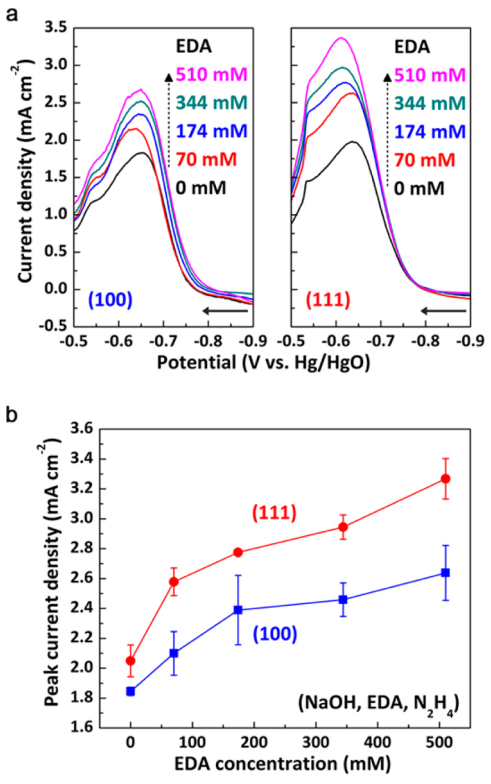

Figure 4. (a) Representative *I*–*V* curves of N_2H_4 oxidation on Cu(100) and Cu(111) electrodes in 15 M NaOH solutions with 5.5 mM N_2H_4 and various concentrations of EDA. The solid black arrows indicate the direction of the linear potential sweeps. (b) Average peak current density of N_2H_4 oxidation according to the concentration of EDA.

DOI: 10.1021/jacs.6b10653
J. Am. Chem. Soc. 2017, 139, 277–284

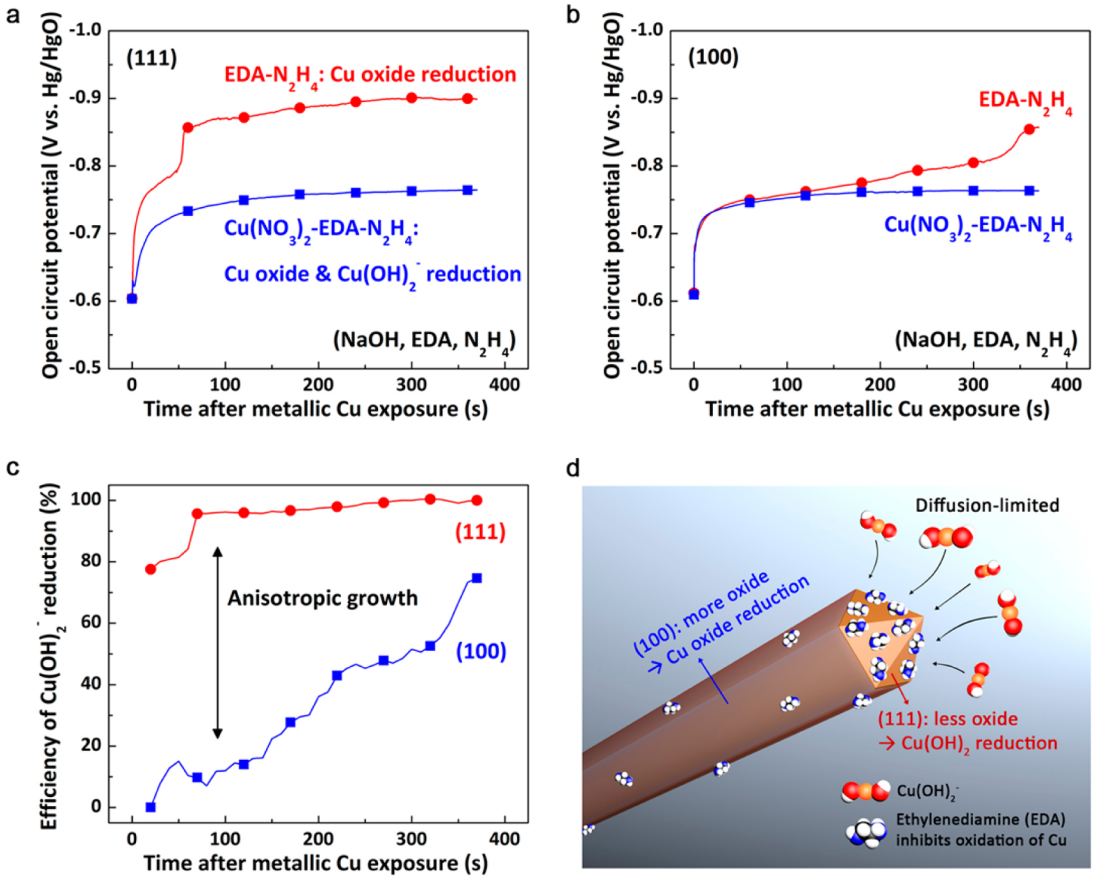

Figure 5. Potential behavior of (a) Cu(111) and (b) Cu(100) crystals in 15 M NaOH solutions containing 70 mM EDA and 5.5 mM N_2H_4 with and without 4.74 mM $Cu(NO_3)_2$. (c) Coulombic efficiency of $Cu(OH)_2^-$ reduction on Cu(111) and Cu(100) surfaces. (d) Schematic diagram of Cu nanowire growth in NaOH–EDA–$Cu(NO_3)_2$–N_2H_4 system.

of a growing Cu nanowire relatively more free of oxide than the (100) facets on the sides of Cu nanowire.

To determine the difference in the reduction rates of $Cu(OH)_2^-$ on Cu(111) and Cu(100) electrodes, we compared the open circuit potential at single-crystal electrodes submerged in NaOH–EDA–N_2H_4 solutions with and without $Cu(NO_3)_2$. The electrons from N_2H_4 oxidation were completely consumed by the reduction of surface oxide in the absence of $Cu(NO_3)_2$ (red circles in Figure 5a,b), but they were consumed by both the reduction of Cu oxide and $Cu(OH)_2^-$ in the solution containing $Cu(NO_3)_2$ (blue squares in Figure 5a,b). Thus, the difference in the potential originates from the reduction of $Cu(OH)_2^-$. As shown in Figure 5a,b, the potential difference between the two solutions was much larger for the Cu(111) (125 mV at 100 s, 138 mV at 300 s) than for the Cu(100) (5 mV at 100 s, 42 mV at 300 s). The Coulombic efficiency of $Cu(OH)_2^-$ reduction was defined as the amount of electrons used for $Cu(OH)_2^-$ reduction divided by the total amount of electrons provided by N_2H_4 (see the Supporting Information). Figure 5c shows that $Cu(OH)_2^-$ reduction was the dominant reaction on Cu(111), whereas oxide reduction was the dominant reaction on Cu(100). This difference between the (111) and (100) facets is responsible for the anisotropic growth of Cu nanowires. This phenomenon originates from the effect of EDA preferentially adsorbing to and inhibiting the oxidation of (111) facets.

We note the facet-selective chemistry is time-dependent in that the Coulombic efficiency of $Cu(OH)_2^-$ reduction on Cu(100) gradually increases over several hundred seconds. It was previously observed that, 300 s after Cu nanowires form, additional Cu can start to deposit on the sides of the nanowires, leading to an increase in the diameter of the nanowires.[48] This phenomenon can now be understood in terms of the increase in the Coulombic efficiency of $Cu(OH)_2^-$ reduction on Cu(100) relative to Cu(111) that occurs over 400 s.

The schematic diagram summarizing our current understanding of EDA-assisted Cu nanowire growth is presented in Figure 5d. The electrons for reduction of both Cu oxide and $Cu(OH)_2^-$ are provided by the oxidation of N_2H_4. The degree to which adsorbed EDA prevents surface oxidation is larger on (111) than that on (100), leading to a larger reduction rate of $Cu(OH)_2^-$ on (111) facets at the end of the nanowire. Meanwhile, Cu oxide is continuously formed via reactions of Cu with OH^- on the (100) facets and continuously reduced by N_2H_4. Thus, rather than acting as a capping agent, EDA acts as an anisotropic promoter of Cu nanowire growth by keeping the facets at the end of the nanowire electrochemically active and free of oxide.

It has previously been hypothesized that the 5-fold twinned crystal structure of metal nanowires plays an important role in inducing anisotropic growth.[49,50] The model for the 5-fold twinned decahedra, five single-crystal tetrahedra oriented radially about a central axis, leaves an unfilled gap of 7.5°. This lack of a space-filling structure is thought to result in strain in the lattice that increases with increasing distance from the central axis of a 5-fold twinned nanowire, which in turn may

DOI: 10.1021/jacs.6b10653
J. Am. Chem. Soc. 2017, 139, 277–284

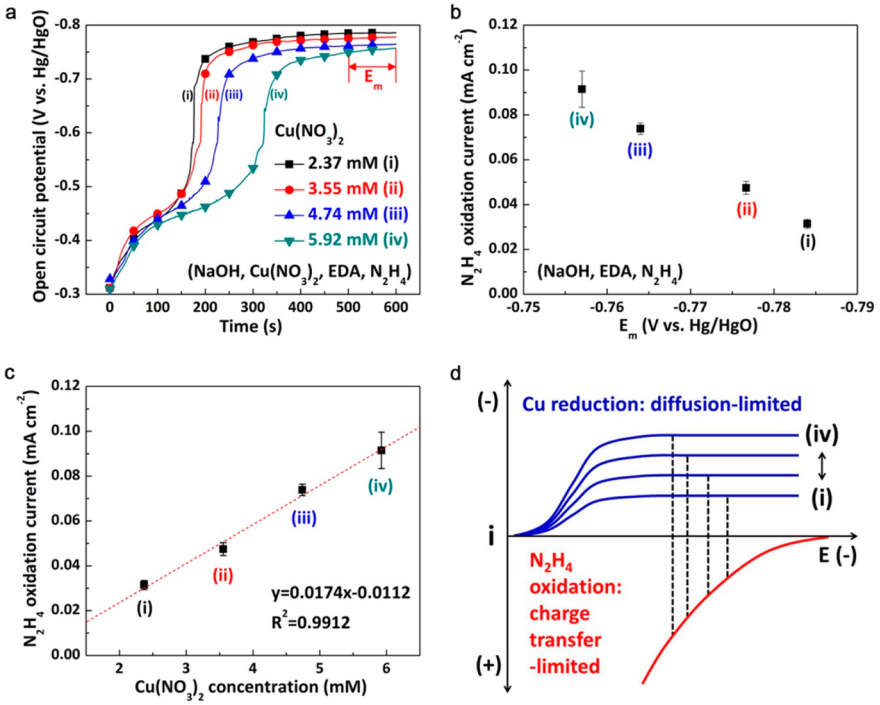

Figure 6. (a) Potential change versus time for the Cu(111) surface in 15 M NaOH solutions with 70 mM EDA, 5.5 mM N_2H_4, and various concentrations of $Cu(NO_3)_2$. (b) Average current density of N_2H_4 oxidation at E_m measured in 15 M NaOH solutions with 70 mM EDA and 5.5–0.25 [$Cu(NO_3)_2$] mM N_2H_4. (c) Correlation between $Cu(NO_3)_2$ concentration and N_2H_4 oxidation current at E_m. (d) Schematic diagram of the I–V curves for diffusion-limited $Cu(OH)_2^-$ reduction and charge transfer-limited N_2H_4 oxidation as a function of the concentration of $Cu(OH)_2^-$.

make lateral growth of nanowires energetically unfavorable.[49] It has also been hypothesized that the twin defects on the ends of the nanowire may serve as active sites for atomic addition.[50] However, these crystal-structure-based mechanistic hypotheses do not explain the time dependence of anisotropic growth in the Cu nanowire system. In contrast, the time scale of the anisotropic efficiency of $Cu(OH)_2^-$ reduction on (111) vs (100) closely matches the time scale over which a change from longitudinal to lateral growth occurs for Cu nanowire growth, resulting in a reduction in aspect ratio of 1810 to 360.[48] Thus, we believe the dominant driving force for anisotropic growth in the EDA-based synthesis of Cu nanowires is the role of EDA in preventing oxidation of the (111) facets at the end of the nanowire; the crystal structure of the nanowire does not appear to play a dominant role. We note that work by Fan and co-workers demonstrating growth of micrometer-sized silver decahedra at low concentrations of polyvinylpyrrolidone (a surface capping agent) also seem to indicate that the strain induced by the 5-fold twinned crystal structure is not sufficient to restrict lateral growth of silver nanowires.[51]

Reduction Rate of $Cu(OH)_2^-$ Is Diffusion-Limited. As a final experiment, we sought to determine whether the reduction of $Cu(OH)_2^-$ onto the Cu(111) surface is limited by charge transfer or the diffusion of $Cu(OH)_2^-$ to the surface. It has previously been determined from real-time observations of Cu nanowire growth that the growth rate of Cu nanowires is diffusion-limited.[40] Thus, this experiment tests to some degree whether our electrochemical system replicates the conditions for nanowire growth. Figure 6a shows the change in open circuit potential at a Cu(111) surface versus time for different concentrations of $Cu(NO_3)_2$. The time for the first polarization was delayed with increasing $Cu(NO_3)_2$ concentration due to the decrease in the amount of remaining N_2H_4 as $Cu(OH)_4^{2-}$ was reduced to $Cu(OH)_2^-$. The E_m for the reaction shifted to a more positive potential as the concentration of $Cu(NO_3)_2$ increased. The oxidation current of N_2H_4 at E_m was measured with chronoamperometry (see Figure S3), and the average oxidation currents are presented in Figure 6b. Figure 6c shows the oxidation rate of N_2H_4 was linearly dependent on the concentration of $Cu(NO_3)_2$ used to obtain the E_m in Figure 6a. As we have confirmed that the adsorption of EDA effectively prevented the formation of surface oxide on Cu(111), the oxidation rate of N_2H_4 at E_m is approximately equal to the rate of Cu deposition. Thus, we conclude that the reduction rate of $Cu(OH)_2^-$ was linearly dependent on the concentration of $Cu(NO_3)_2$.

The schematic diagram for the diffusion-limited reduction of $Cu(OH)_2^-$ (blue line) and charge transfer-limited oxidation of N_2H_4 (red line) at various concentrations of $Cu(NO_3)_2$ is presented in Figure 6d. The opposite case, i.e., charge transfer-limited reduction of $Cu(OH)_2^-$ and diffusion-limited oxidation of N_2H_4, is shown in Figure S4. A diffusion-limited reaction is one in which the rate-determining step is the diffusion of reactants; thus, the reaction rate is dependent on the concentration of reactants, not the electrode potential. In contrast, the applied potential determines the rate of a charge transfer-limited reaction.[52] The points at which the dashed line crosses the *x*-axis in both figures corresponds to E_m where the rates of the redox reactions are identical. As illustrated in Figure 6d, if the reduction of $Cu(OH)_2^-$ is diffusion-limited, we would expect that the reaction rate increases linearly and E_m shifts to more positive potentials as the concentration of $Cu(NO_3)_2$ increases. This prediction matches the experimental observations in Figure 6a,c. In contrast, the rate of the charge transfer-limited reduction of $Cu(OH)_2^-$ would be constant regardless of $Cu(NO_3)_2$ concentration (see Figure S4). Thus, we conclude

DOI: 10.1021/jacs.6b10653
J. Am. Chem. Soc. 2017, 139, 277–284

that the electrochemical reactions on the Cu(111) surface consist of diffusion-limited reduction of $Cu(OH)_2^-$ and charge transfer-limited oxidation of N_2H_4. This conclusion agrees with previous results from the real-time visualization of Cu nanowire growth that show the growth rate of Cu nanowires was linearly dependent on the concentration of $Cu(NO_3)_2$.[40]

CONCLUSIONS

We showed that EDA, a so-called capping agent in the synthesis of Cu nanowires, is actually a facet-selective promoter of Cu atomic addition to the (111) facets at the end of a Cu nanowire. Measurements with an electrochemical quartz crystal microbalance demonstrated that only 25% of electrons from N_2H_4 oxidation go toward reduction of $Cu(OH)_2^-$ to metallic Cu; the remainder are consumed by the reduction of Cu oxides that are continuously formed due to the high pH environment. By comparing the rate of Cu oxide reduction on Cu(111) and Cu(100) surfaces, we showed that EDA passivates Cu(111) against further oxidation more quickly than for Cu(100). Although EDA passivates Cu(111) from oxidation, it actually promotes N_2H_4 oxidation on Cu surfaces, likely by keeping the Cu surface metallic and relatively free of oxides. The EDA-enhanced passivation of the Cu(111) surface opens a ~300 s window during which anisotropic growth of Cu nanowires can occur. If the Cu nanowire reaction continues outside of this window, Cu nanowires can grow laterally, resulting in larger nanowire diameters.[48] The series of electrochemical experiments in this article can likely be applied to a wide variety of metal nanostructure syntheses to determine the precise role of so-called capping agents and thereby greatly improve the understanding of how anisotropic growth of metal nanostructures occurs.

ASSOCIATED CONTENT

Supporting Information

The Supporting Information is available free of charge on the ACS Publications website at DOI: 10.1021/jacs.6b10653.

Experimental methods and calculations and additional results of electrochemical analyses (PDF)

AUTHOR INFORMATION

Corresponding Author

*benjamin.wiley@duke.edu

ORCID

Benjamin J. Wiley: 0000-0003-0055-9018

Notes

The authors declare no competing financial interest.

ACKNOWLEDGMENTS

This work was supported by a National Science Foundation CAREER award (DMR-1253534) and the "R&D Center for Reduction of Non-CO_2 Greenhouse Gases (2013001690004)" funded by the Korea Ministry of Environment (MOE) as a "Global Top Environment R&D Program".

REFERENCES

(1) Jana, N. R.; Gearheart, L.; Murphy, C. J. *J. Phys. Chem. B* **2001**, *105*, 4065−4067.
(2) Xia, Y.; Yang, P.; Sun, Y.; Wu, Y.; Mayers, B.; Gates, B.; Yin, Y.; Kim, F.; Yan, H. *Adv. Mater.* **2003**, *15*, 353−389.
(3) Tao, A.; Kim, F.; Hess, C.; Goldberger, J.; He, R.; Sun, Y.; Xia, Y.; Yang, P. *Nano Lett.* **2003**, *3*, 1229−1233.
(4) Murphy, C. J.; Sau, T. K.; Gole, A. M.; Orendorff, C. J.; Gao, J.; Gou, L.; Hunyadi, S. E.; Li, T. *J. Phys. Chem. B* **2005**, *109*, 13857−13870.
(5) Wiley, B. J.; Sun, Y.; Xia, Y. *Acc. Chem. Res.* **2007**, *40*, 1067−1076.
(6) Huo, Z.; Tsung, C.-K.; Huang, W.; Zhang, X.; Yang, P. *Nano Lett.* **2008**, *8*, 2041−2044.
(7) Wang, C.; Hu, Y.; Lieber, C. M.; Sun, S. *J. Am. Chem. Soc.* **2008**, *130*, 8902−8903.
(8) Yun, S.; Niu, X.; Yu, Z.; Hu, W.; Brochu, P.; Pei, Q. *Adv. Mater.* **2012**, *24*, 1321−1327.
(9) Hsu, P.-C.; Liu, X.; Liu, C.; Xie, X.; Lee, H. R.; Welch, A. J.; Zhao, T.; Cui, Y. *Nano Lett.* **2015**, *15*, 365−371.
(10) Ye, S.; Rathmell, A. R.; Chen, Z.; Stewart, I. E.; Wiley, B. J. *Adv. Mater.* **2014**, *26*, 6670−6687.
(11) Bhanushali, S.; Ghosh, P.; Ganesh, A.; Cheng, W. *Small* **2015**, *11*, 1232−1252.
(12) Kumar, D. V. R.; Woo, K.; Moon, J. *Nanoscale* **2015**, *7*, 17195−17210.
(13) Zhang, D.; Wang, R.; Wen, M.; Weng, D.; Cui, X.; Sun, J.; Li, H.; Lu, Y. *J. Am. Chem. Soc.* **2012**, *134*, 14283−14286.
(14) Wu, H.; Kong, D.; Ruan, Z.; Hsu, P.-C.; Wang, S.; Yu, Z.; Carney, T. J.; Hu, L.; Fan, S.; Cui, Y. *Nat. Nanotechnol.* **2013**, *8*, 421−425.
(15) Cui, F.; Yu, Y.; Dou, L.; Sun, J.; Yang, Q.; Schildknecht, C.; Schierle-Arndt, K.; Yang, P. *Nano Lett.* **2015**, *15*, 7610−7615.
(16) Won, Y.; Kim, A.; Lee, D.; Yang, W.; Woo, K.; Jeong, S.; Moon, J. *NPG Asia Mater.* **2014**, *6*, e105.
(17) Sachse, C.; Weiß, N.; Gaponik, N.; Müller-Meskamp, L.; Eychmüller, A.; Leo, K. *Adv. Energy Mater.* **2014**, *4*, 1300737.
(18) Im, H.-G.; Jung, S.-H.; Jin, J.; Lee, D.; Lee, J.; Lee, D.; Lee, J.-Y.; Kim, I.-D.; Bae, B.-S. *ACS Nano* **2014**, *8*, 10973−10979.
(19) Tang, Y.; Gong, S.; Chen, Y.; Yap, L. W.; Cheng, W. *ACS Nano* **2014**, *8*, 5707−5714.
(20) Hsu, P.-C.; Wang, S.; Wu, H.; Narasimhan, V. K.; Kong, D.; Lee, H. R.; Cui, Y. *Nat. Commun.* **2013**, *4*, 2522.
(21) Hu, W.; Wang, R.; Lu, Y.; Pei, Q. *J. Mater. Chem. C* **2014**, *2*, 1298−1305.
(22) Song, J.; Li, J.; Xu, J.; Zeng, H. *Nano Lett.* **2014**, *14*, 6298−6305.
(23) Taberna, P. L.; Mitra, S.; Poizot, P.; Simon, P.; Tarascon, J.-M. *Nat. Mater.* **2006**, *5*, 567−573.
(24) Cao, F.-F.; Deng, J.-W.; Xin, S.; Ji, H.-X.; Schmidt, O. G.; Wan, L.-J.; Guo, Y.-G. *Adv. Mater.* **2011**, *23*, 4415−4420.
(25) Lu, L.-L.; Ge, J.; Yang, J.-N.; Chen, S.-M.; Yao, H.-B.; Zhou, F.; Yu, S.-H. *Nano Lett.* **2016**, *16*, 4431−4437.
(26) Chen, Z.; Ye, S.; Wilson, A. R.; Ha, Y.-C.; Wiley, B. J. *Energy Environ. Sci.* **2014**, *7*, 1461−1467.
(27) Raciti, D.; Livi, K. J.; Wang, C. *Nano Lett.* **2015**, *15*, 6829−6835.
(28) Alia, S. M.; Pivovar, B. S.; Yan, Y. *J. Am. Chem. Soc.* **2013**, *135*, 13473−13478.
(29) Fan, Z.; Liu, B.; Liu, X.; Li, Z.; Wang, H.; Yang, S.; Wang, J. *Electrochim. Acta* **2013**, *109*, 602−608.
(30) Choi, H.; Park, S.-H. *J. Am. Chem. Soc.* **2004**, *126*, 6248−6249.
(31) Gerein, N. J.; Haber, J. A. *J. Phys. Chem. B* **2005**, *109*, 17372−17385.
(32) Wu, H.; Hu, L.; Rowell, M. W.; Kong, D.; Cha, J. J.; McDonough, J. R.; Zhu, J.; Yang, Y.; McGehee, M. D.; Cui, Y. *Nano Lett.* **2010**, *10*, 4242−4248.
(33) Liu, Z.; Yang, Y.; Liang, J.; Hu, Z.; Li, S.; Peng, S.; Qian, Y. *J. Phys. Chem. B* **2003**, *107*, 12658−12661.
(34) Chang, Y.; Lye, M. L.; Zeng, H. C. *Langmuir* **2005**, *21*, 3746−3748.
(35) Rathmell, A. R.; Bergin, S. M.; Hua, Y.-L.; Li, Z.-Y.; Wiley, B. J. *Adv. Mater.* **2010**, *22*, 3558−3563.
(36) Jin, M.; He, G.; Zhang, H.; Zeng, J.; Xie, Z.; Xia, Y. *Angew. Chem., Int. Ed.* **2011**, *50*, 10560−10564.
(37) Liu, Z.; Chen, Y.; Zheng, Y. *CrystEngComm* **2014**, *16*, 9054−9062.
(38) Chen, J.; Chen, J.; Li, Y.; Zhou, W.; Feng, X.; Huang, Q.; Zheng, J.-G.; Liu, R.; Ma, Y.; Huang, W. *Nanoscale* **2015**, *7*, 16874−16879.

DOI: 10.1021/jacs.6b10653
J. Am. Chem. Soc. 2017, 139, 277−284

(39) Koo, J.; Kwon, S.; Kim, N. R.; Shin, K.; Lee, H. M. *J. Phys. Chem. C* **2016**, *120*, 3334−3340.
(40) Ye, S.; Chen, Z.; Ha, Y.-C.; Wiley, B. J. *Nano Lett.* **2014**, *14*, 4671−4676.
(41) Mohl, M.; Pusztai, P.; Kukovecz, A.; Konya, Z.; et al. *Langmuir* **2010**, *26*, 16496−16502.
(42) Liu, Y.-Q.; Zhang, M.; Wang, F.-X.; Pan, G.-B. *RSC Adv.* **2012**, *2*, 11235−11237.
(43) Xu, W.-H.; Wang, L.; Guo, Z.; Chen, X.; Liu, J.; Huang, X.-J. *ACS Nano* **2015**, *9*, 241−250.
(44) Singh, D. P.; Ojha, A. K.; Srivastava, O. N. *J. Phys. Chem. C* **2009**, *113*, 3409−3418.
(45) Karim-Nezhad, G.; Jafarloo, R.; Dorraji, P. S. *Electrochim. Acta* **2009**, *54*, 5721−5726.
(46) Bindra, P.; Light, D.; Rath, D. *IBM J. Res. Dev.* **1984**, *28*, 668−678.
(47) Feldman, B. J.; Melroy, O. R. *J. Electrochem. Soc.* **1989**, *136*, 640−643.
(48) Ye, S.; Rathmell, A. R.; Stewart, I. E.; Ha, Y.-C.; Wilson, A. R.; Chen, Z.; Wiley, B. J. *Chem. Commun.* **2014**, *50*, 2562−2564.
(49) Lofton, C.; Sigmund, W. *Adv. Funct. Mater.* **2005**, *15*, 1197−1208.
(50) Chen, J.; Wiley, B. J.; Xia, Y. *Langmuir* **2007**, *23*, 4120−4129.
(51) Zhang, W.; Liu, Y.; Cao, R.; Li, Z.; Zhang, Y.; Tang, Y.; Fan, K. *J. Am. Chem. Soc.* **2008**, *130*, 15581−15588.
(52) Bard, A. J.; Faulkner, L. R. *Electrochemical Methods*, 2nd ed.; John Wiley & Sons: New York, 2001.

DOI: 10.1021/jacs.6b10653
J. Am. Chem. Soc. 2017, 139, 277−284